

## Thermoplasmonic of Single Au@SiO<sub>2</sub> and SiO<sub>2</sub>@Au Core Shell Nanoparticles in Deionized Water and Poly-vinylpyrrolidoneMatrix

Maher Abdulfadhil Gatea

Hussein A. Jawad\*

Received 18/6/2018, Accepted 22/11/2018, Published 2/6/2019

This work is licensed under a [Creative Commons Attribution 4.0 International License](#).

### Abstract:

Metal nanoparticles can serve as an efficient nano-heat source with confinement photothermal effects. Thermo-plasmonic technology allows researchers to control the temperature at a nanoscale due to the possibility of precise light propagation. The response of opto-thermal generation of single gold-silica core-shell nanoparticle immersed in water and Poly-vinylpyrrolidone surrounding media is theoretically investigated. Two lasers (CW and fs pulses) at the plasmonic resonance (532 nm) are utilized. For this purpose, finite element method is used via COMSOL multiphysics to find a numerical computation of absorption cross section for the proposed core –shell NP in different media. Thermo-plasmonic response for both lasers is studied. The heat profile of different nanostructures is estimated. The results revealed that the temperature distribution profile was varied due to changing in the relative volume fraction between the core and the shell of nanoparticle.

**Key words:** Core-shell nanoparticle, COMSOL multiphysics, Gold nanoparticles, PVP, Thermoplasmonic.

### Introduction:

The thermo-plasmonic field combines nano-thermodynamics and nano-optics (1). It focuses on absorption of optical energy and then converted into controllable a nano-source of heat. The amount of heat generated reaches its maximum value when the optical radiation at the surface plasmon resonance (SPR) wavelength. Heat nano-source with confined distribution could be used for wide range of application such as biomedical treatment (2) photoacoustic imaging (3), gene and drug delivery (4), and plasma-fluidics (5).

The primary challenge of thermo-plasmonic technology regards the design of micro/nanoscale particles and the dissipation of heat measurements (6). Noble metals have a distinguished surface plasmon resonance when it is illuminated by optical radiation resonant with their surface plasmon oscillation. They absorb the energy of optical radiation and convert it into heat through photophysical processes (7) by three time step processes: first, electronic absorption, second electron-phonon thermalization, and third, the heat is diffused to the surrounding media (8). The rate of absorption and laser power are controllable where they affect directly on the rate of generated heat by nanoparticles (9).

Institute of Laser for Postgraduate Studies, University of Baghdad, Baghdad, Iraq.

\*Corresponding author: [Hussein@ilps.uobaghdad.edu.iq](mailto:Hussein@ilps.uobaghdad.edu.iq)

Noble metals are extensively used as plasmonic nano-heat source with wide wavelength range illumination as well as different exposure times (10- 14). Surface plasmon resonance exhibits high tunability in case of core-shell nanoparticles among various metallic nanostructures due to the sensitivity of SPR to nanostructures' sizes, shapes, and environments (15).

The silica shell acts as a tool to control the distance between metal particles. In addition, it has the ability to enhance SPR tunability and metal colloidal stability in water (16). The used surrounding media are dependent on the applications. For example the water is analogous to the living tissue of the medical field (10). Mean while, the transparent polymer Polyvinylpyrrolidone (PVP) provide high stabilize environment prevent aggregation of core shell NP's (17).

In this article, the finite element method using COMSOL multiphysics based on Drude-Lorentz model and heat transfer model is used to investigate the heat transferred from spherical core shell nanoparticle that illuminated by CW and fs laser radiation to the surrounding media.

### Structure and simulation:

Spherical symmetry of core- shell nanoparticles of core radius "R" and shell thickness "d", Au@SiO<sub>2</sub> NP and SiO<sub>2</sub>@Au NP. The core

radius (10,20,30,40) nm was used while the shell thickness used is only 5 nm , then 20 nm core radius was used with (10,20,30,40) nm of shell thickness. They immersed in two suspensions, homogeneous deionized water and PVP. The core shell NPs were irradiated by two laser sources, 532 nm cwNd:YAG and 86 MHz fs Nd:YAG lasers with the irradiance of 1 (mW/um<sup>2</sup>) for both.

#### Numerical simulation:

A- Optical part: COMSOL multiphysics 5.3a was utilized to find a numerical computation of the absorption cross-section for the proposed core – shell NP in different media, where the thickness of the Perfectly Matched Layer (PML)was  $\lambda/2$ .The symmetry of a quarter sphere is only considered from the simulation geometry for the simplicity(18) as shown in Fig.(1).

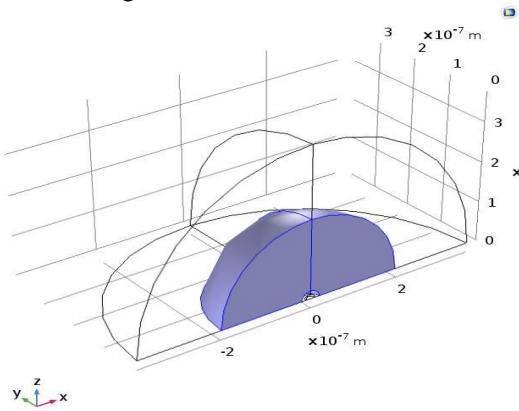


**Figure 1.**Geometrical structure of one quarter of the core shell nanoparticle in homogeneous liquid medium.

High mesh quality of  $\lambda/6$  was selected in this model. Real and imaginary components of the refractive indices of all materials (air (19), water (20), PVP (21)) (gold (22) and silica (23)) were interpolated.

The relative permittivity is

$$\epsilon_r = (n - ik)^2 \dots 1$$

Both the absorption and scattering cross sections mainly depend on the polarizability ( $\alpha$ ) of the nanosphere (24).

$$\alpha = \frac{4\pi R^3(\epsilon_{Au} - \epsilon_{med})}{(\epsilon_{Au} + \epsilon_{med})} \dots 2$$

where  $\epsilon_{Au}$  and  $\epsilon_{med}$  are the dielectric constant of Au and surrounding medium respectively.

Then the absorption cross section is given by(25)

$$\sigma_{acs} = k Im(\alpha) - \frac{k^4/\alpha^2}{6\pi} \dots 3$$

Thermal Analysis: the photo-thermal response of plasmonic core - shell NP's which arise from absorption of incident light energy was investigated using COMSOL 5.3a Multiphysics. The time depending of the heat transfer model was used with same boundary conditions that used to find the optical properties. The properties of the used material are shown in Table (1).

**Table 1.**physical constant of material used in this article.

Parameters	Au	SiO <sub>2</sub>	Water	PVP	Unit
Thermal conductivity $k$	317	1.4	0.6	2.8	W/(m·K)
Specific heat capacity $c$	128.5	730	4187	3428	J/(kg·K)
Mass density $\rho$	19320	2200	1000	1200	kg/m <sup>3</sup>

The nanoparticle temperature under irradiation of CW laser illumination in the effective volume (26)

$$T^{cw}(r) = \frac{I \sigma_{acs}}{4\pi k_{med} r} (1 + \lambda_K) \dots \dots \dots \text{for } r > R \dots 4$$

where

$I \sigma_{acs} = Q$  is the heat power.

$r$  is the position distance.

$k_{med}$  thermal conductivity of surrounding media (water , PVP).

The nanoparticle temperature under irradiation of fs laser pulse is:

$$T^{fs} = \frac{I^* \sigma_{acs}}{\rho_{Au} c_{Au} V} \dots 5$$

Where

$I^*$  is laser average irradiance,  $V$  is the nanoparticle volume.

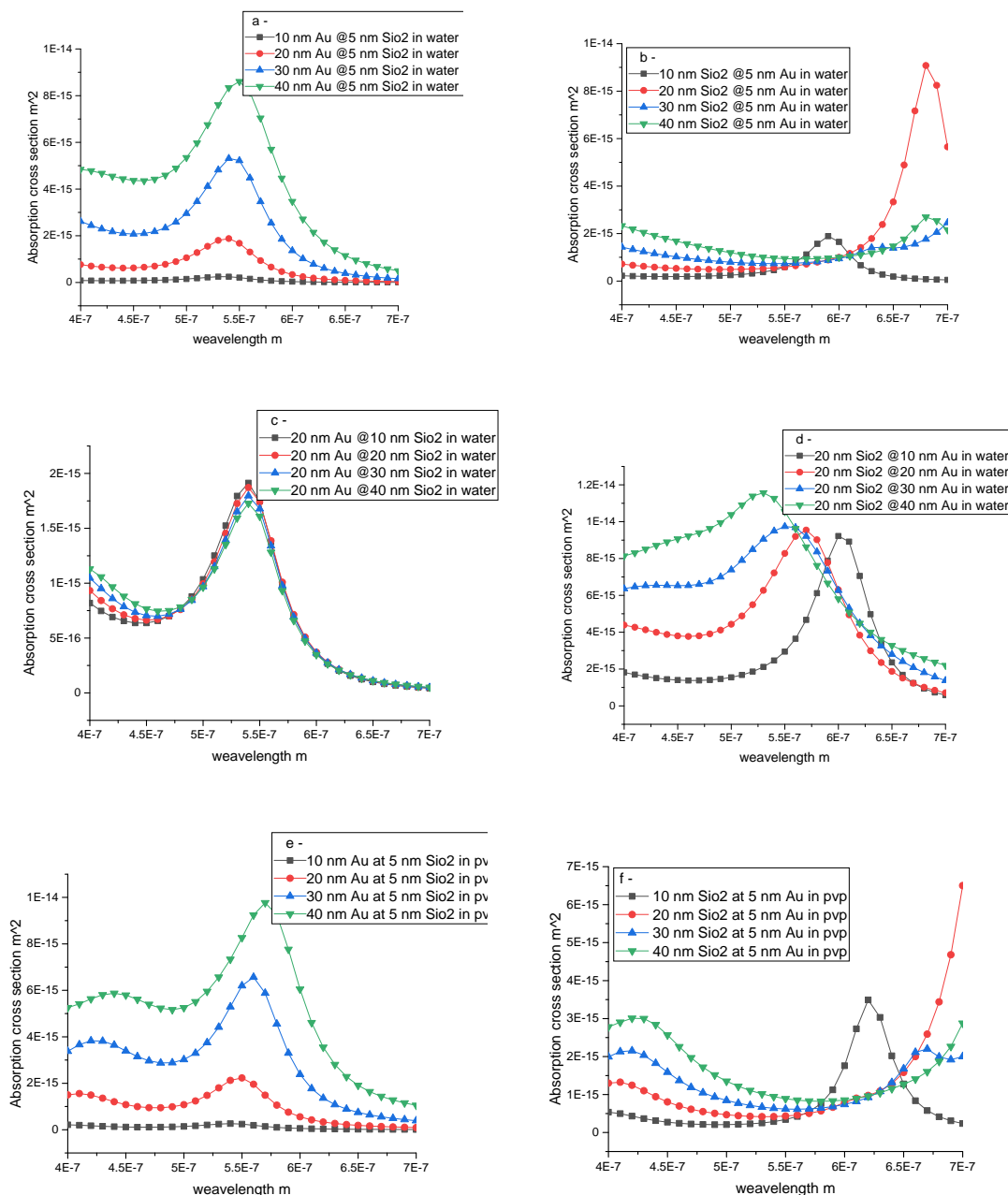
The generated heat power is considered to be uniform inside the NP because the thermal conductivity of the metals is much larger than that of the surroundings (27).

#### Results and Discussion:

Figure 2 (a,e) shows the absorption cross section as a function of wavelength(400-700) nm for different Au core diameter at 5 nm of SiO<sub>2</sub> shell thickness in water and PVP matrix surroundings.

The SPR characteristics show small red shifts and increases the absorption cross section magnitude with increasing the Au core radius because the increment of the relative refractive index of the NPs (28). When the SiO<sub>2</sub> is used as a core instead of Au both SPR characteristics reveal a clear red shift with increasing of SiO<sub>2</sub> core radius as shown in Fig 2(b,f).

If the core radius is fixed and the variation in the shell thickness, Fig 2 (c,g) shows the absorption cross-section as a function of wavelength for 20 nm Au core diameter at different  $\text{SiO}_2$  shell thickness in water and PVP matrix surroundings. Both SPR characteristics exhibit a decreasing absorption cross-section with increasing the  $\text{SiO}_2$  shell thickness. While in case of  $\text{SiO}_2$  is used as a core instead of Au , a blue shift was observed with increasing the Au shell thickness as shown in Fig 2



(d,h) which is in agreement with the spectral results of Qiang Li (10).

Fig 2 (a,c,e,g) shows that the absorption cross-section peaks are close to the excitation wavelength (532 nm), which get it a suitable structure to generate higher amount of photothermal heat compared to other structures. The generation of heat by NP mainly depends on the amount of absorption cross-section (eqs 4,5).

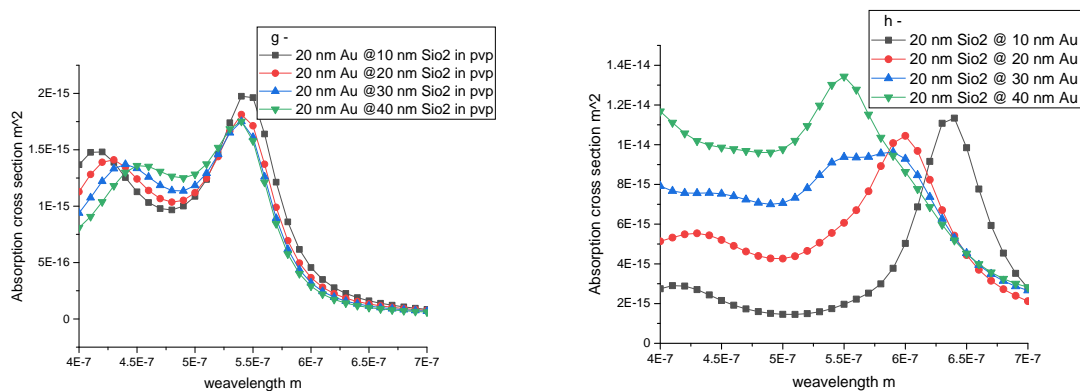
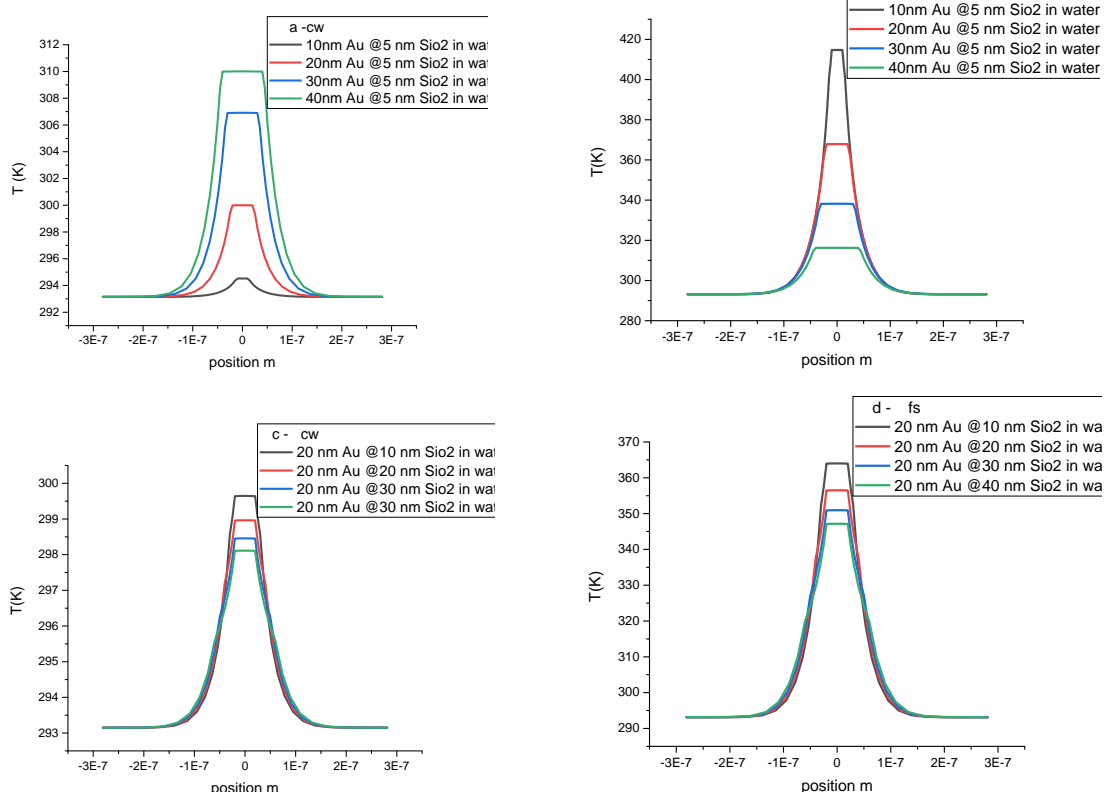


**Figure 2** Absorption cross section as a function of wavelength for:  
a-Au at SiO<sub>2</sub> in water b-SiO<sub>2</sub> at Au in water c-20nm Au at different radius of SiO<sub>2</sub> in water d- 20nm SiO<sub>2</sub> at different radius of Au in water e- Au at SiO<sub>2</sub> in PVP f- SiO<sub>2</sub> at Au in PVP g-20nm Au at different radius of SiO<sub>2</sub> in PVP h-20nm SiO<sub>2</sub> at different radius of Au in PVP

Normal incident of 532 nm CW and Fs lasers on core-shell NPs and the temperature distribution of different volume fraction material in water and PVP surrounding media are shown in Fig. 3. In the case of CW illumination, Fig. 3 (a,e) showed that the temperature elevated and the radial thermal profile broadened with the increment of Au core diameter, while Fig. 3 (c,g) showed that the elevated temperature inversely proportional to the increase in SiO<sub>2</sub> shell thickness depending on their absorption cross section behavior. The temperature

rise in the cases of Fig. 2 (b,d,f,h) is not considered because small absorption cross section at the expatiation wavelength.

In the case of fs laser pulse illumination, the generated temperature for the proposed core shell structure in both surrounding media get much enhanced by increasing the particle core diameter as shown in Fig. 3 (b,f) with high radial heat confinement, while Fig. 3 (d,h) revealed clear decreasing with the increase of SiO<sub>2</sub> shell thickness.



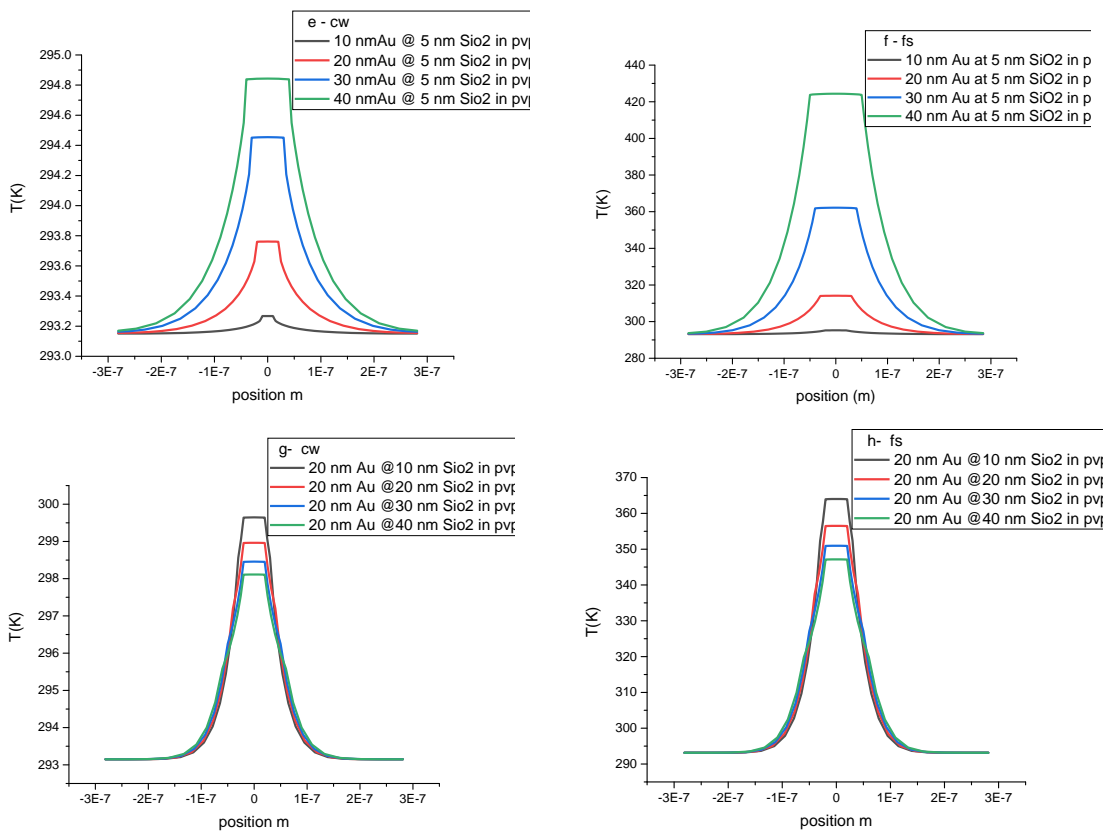


**Figure 3 Heat dissipation as a function of distance from the NP center of a-Au at SiO<sub>2</sub> in water (CW) b- Au at SiO<sub>2</sub> in water(fs) c-20nm Au at different radius of SiO<sub>2</sub> in water(CW) d- 20nm Au at different radius of SiO<sub>2</sub> in water(fs) e- Au at SiO<sub>2</sub> in PVP(CW) f- Au at SiO<sub>2</sub> in PVP(fs) g-20nm Au at different radius of SiO<sub>2</sub> in PVP(CW) h-20nm Au at different radius of SiO<sub>2</sub> in PVP(fs)**

Different SiO<sub>2</sub> shell thicknesses have a clear effect on the maximum temperature elevation of NPs, but does not affect the temperature distribution to the surrounding media as shown in Fig. 3 (c,d,g,h). The same behavior could be seen in the result of G.Baffou (24). The fs-laser illumination provided higher radial heat confinement compared to CW radiation, (more than 50 nm) as shown in Fig 3 (a,b,e,f). This heat confinement is due to the short pulse duration which does not give enough time to the heat to be dissipated (27).

### Conclusions:

In conclusion, the simulated results of CW and pulse thermo-plasmonic response is perform for a single gold-silica core shell NP with different relative volume fraction of the core and the shell parts using finite element method by COMSOL multiphysics. In the case of CW laser illumination of Au @ SiO<sub>2</sub>, the elevated temperature is proportional to the increase of the core radius. In contrast, the temperature decreased in the fs laser. The generated temperature of NP decreases with increases the thickness of SiO<sub>2</sub> shell in both lasers at fixed core radius (20 nm).

### Acknowledgements:

This work was supported by Institute of Laser for Postgraduate Studies, University of Baghdad, Baghdad, Iraq.

### Conflicts of Interest: None.

### References:

1. Osman N M. Polypyrrole as a thermoplasmonic. ICCNEEE.2015.
2. Abadeer NS, Murphy CJ. Recent progress in cancer thermal therapy using gold nanoparticles. J Phys Chem. C. 2016 Feb 26;120(9):4691-716.
3. Zhang Q, Iwakuma N, Delano M, Sharma P, Wu C, Mcneil J, et al. Gold Nanoparticles as Contrast Agent for in vivo Photoacoustic Tomography of Tumor. J Biomed Opt. Sep3,20(2009);395102(8pp)
4. Rwei AY, Wang W, Kohane DS. Photoresponsive nanoparticles for drug delivery. Nano today. 2015 Aug 1;10(4):451-67.
5. Zhao C, Liu Y, Zhao Y, Fang N, Huang TJ. A reconfigurable plasmonofluidic lens. Nat Commun. 2013 Aug 9;4:2305.
6. Coppens ZJ, Li W, Walker DG, Valentine JG. Probing and controlling photothermal heat generation in plasmonic nanostructures. Nano Lett. 2013 Mar 1;13(3):1023-8.

7. Khurgin JB, Sun G, Chen WT, Tsai WY, Tsai DP. Ultrafast thermal nonlinearity. *Sci Rep.* 2015 Dec 8;5:17899.
8. Baffou G, Quidant R. Thermo-plasmonics: using metallic nanostructures as nano-sources of heat. *Laser & Photonics Reviews.* 2013 Mar;7(2):171-87.
9. Zhu J. Surface plasmon resonance from bimetallic interface in Au–Ag core–shell structure nanowires. *Nanoscale Res Lett.* 2009 Sep 1;4(9):977.
10. Li Q, Zhang W, Zhao D, Qiu M. Photothermal enhancement in core-shell structured plasmonic nanoparticles. *Plasmonics.* 2014 Jun 1;9(3):623-30.
11. Shen S, Wang S, Zheng R, Zhu X, Jiang X, Fu D, et.al. Magnetic nanoparticle clusters for photothermal therapy with near-infrared irradiation. *Biomaterials.* 2015 Jan 1;39:67-74.
12. Norton SJ, Vo-Dinh T. Photothermal effects of plasmonic metal nanoparticles in a fluid. *J Appl Phys.* 2016 Feb 28;119(8):083105.
13. Howard TV, Dunklin JR, Forcherio GT, Roper DK. Thermoplasmonic dissipation in gold nanoparticle–polyvinylpyrrolidone thin films. *RSC Advances.* 2017;7(89):56463-70.
14. Shi Y, Yang S, Xing D. Quantifying the plasmonic nanoparticle size effect on photoacoustic conversion efficiency. *J Phys Chem. C.* 2017 Mar 3;121(10):5805-11
15. Zheng YB, Huang TJ, Desai AY, Wang SJ, Tan LK, Gao H, et.al.. Thermal behavior of localized surface plasmon resonance of Au/ Ti O<sub>2</sub> core/shell nanoparticle arrays. *Appl Phys Lett.* 2007 Apr 30;90(18):183117.
16. Ghosh Chaudhuri R, Paria S. Core/shell nanoparticles: classes, properties, synthesis mechanisms, characterization, and applications. *Chem Rev.* 2011 Dec 28;112(4):2373-433.
17. Zhang Z, Sèbe G, Wang X, Tam KC. Gold nanoparticles stabilized by poly (4-vinylpyridine) grafted cellulose nanocrystals as efficient and recyclable catalysts. *Carbohydromol.* 2018 Feb 15;182:61-8.
18. Devi J, Saikia R, Datta P. Modeling of absorption and scattering properties of core -shell nanoparticles for application as nanoantenna in optical domain. *JPCS.* 2016;759, 012039.
19. Ciddor PE. Refractive index of air: new equations for the visible and near infrared. *Appl Opt.* 1996 Mar 20;35(9):1566-73.
20. Hale GM, Querry MR. Optical constants of water in the 200-nm to 200-μm wavelength region. *Appl opt.* 1973 Mar 1;12(3):555-63.
21. König TA, Ledin PA, Kerszulis J, Mahmoud MA, El-Sayed MA, Reynolds JR, et.al. Electrically tunable plasmonic behavior of nanocube–polymer nanomaterials induced by a redox-active electrochromic polymer. *ACS nano.* 2014 Jun 3;8(6):6182-92.
22. Johnson PB, Christy RW. Optical constants of the noble metals. *Phys Rev B.* 1972 Dec 15;6(12):4370.
23. Gao L, Lemarchand F, Lequime M. Refractive index determination of SiO<sub>2</sub> layer in the UV/Vis/NIR range: spectrophotometric reverse engineering on single and bi-layer designs. *JEOS.* Jan 31,8(2013) 13010(8pp)
24. Baffou G, Quidant R, Girard C. Thermoplasmonics modeling: A Green's function approach. *Phys Rev B.* 2010 Oct 13;82(16):165424.
25. Hamidi SM, Oskuei MA. Adjustable surface plasmon resonance with Au, Ag, and Ag@ Au core-shell nanoparticles. *COL.* 2014 Mar 1;12(3):031601.
26. Baffou G, Quidant R, García de Abajo FJ. Nanoscale control of optical heating in complex plasmonic systems. *ACS nano.* 2010 Jan 7;4(2):709-16.
27. Baffou G, Rigneault H. Femtosecond-pulsed optical heating of gold nanoparticles. *Phys Rev B.* 2011 Jul 21;84(3):035415.
28. Shi Y, Yang S, Xing D. Quantifying the plasmonic nanoparticle size effect on photoacoustic conversion efficiency. *J Phys Chem. C.* 2017 Mar 3;121(10):5805-11.

## الحرارة البلازمونية لجسيم نانوي مفرد من الذهب وقشرة (ذهب وسليكا) في محيط مائي وبوليمر من نوع pvp

حسين علي جواد

ماهر عبد الفاضل كاطع

معهد الليزر للدراسات العليا، جامعة بغداد، بغداد، العراق.

### الخلاصة:

الجسيمات النانوية المعدنية كمصدر حراري نانوي فعال في حصر الحرارة الضوئية اجتذب مختلف التطبيقات. البلازمون - الحراري تسمح بالسيطرة على درجة الحرارة في المدى النانوي بسبب إمكانية دقة انتشار الضوء تمت الدراسة النظرية للاستجابة الحرارية البصرية المتولدة من جسيم نانوي متكون من الذهب وقشرة للذهب والسليكا المغمورة في محيط مائي وبوليمر من نوع pvp. استخدم نوعين من الليزرات أحدهما مستمر والآخر نبضي في امد الفيمتو ثانية يعملان بالطول الموجي الرئيسي (532 نانومتر). استخدم لهذا الغرض برنامج محركات حاسوبي المسمى COMSOL multiphysics لإيجاد المقطع العرضي للامتصاص للجسيمات النانوية المفترضة من الذهب والقشرة في مختلف الأوساط بحسب الاستجابة الحرارية البلازمونية لكلا الليزرین. تم تحديد الشكل المتوقع للحرارة المتولدة من مختلف الجسيمات النانوية. اظهرت النتائج ان شكل التوزيع الحراري تغير طبقا الى تغير الحجم النسبي بين الذهب والقشرة للجسيمات النانوية.

**الكلمات المفتاحية :** جسيمات نانوية من الذهب وقشرة، جسيمات الذهب النانوية، بولمر PVP، برنامج COMSOL، الحرارة البلازمونية .